投稿論文(英文)
PAPERS

J. Materials, Conc. Struct., Pavements No. 520/V-28, 273-286, August 1995

FINITE ELEMENT ANALYSIS ON SHEAR RESISTING MECHANISM OF CONCRETE BEAMS WITH SHEAR REINFORCEMENT

Tamon UEDA[1], Nares PANTARATORN[2] and Yasuhiko SATO[3]

[1]Member of JSCE, Dr. Eng., Associate Professor, Department of Civil Engineering, Hokkaido University
(Nishi 8, Kita 13, Kita-ku, Sapporo 060, Japan)
[2]Dr. Eng., Head, Department of Civil Engineering, Sripatum University
(61 Phahonyothin Rd., Jatujak, Bangkok 10900, Thailand)
[3]Member of JSCE, Dr. Eng., Research Associate, Department of Civil Engineering, Hokkaido University
(Nishi 8, Kita 13, Kita-ku, Sapporo 060 Japan)

The nonlinear finite element analysis program for reinforced concrete planar member subjected to reversed cyclic loading is expanded to analyze reinforced and prestressed concrete linear members with shear reinforcement subjected to one-sided cyclic loading. It is found that the predicted strains of shear reinforcement can be made much closer to the experimental ones by considering reduction of concrete tension stiffness due to slip of shear reinforcement at its lower bent. The ultimate strengths of beams are also predicted reasonably. Based on the analysis, a new truss model is presented to explain shear resisting mechanism of beams with shear reinforcement.

Key Words : *shear, shear resisting mechanism, reinforced concrete beam, prestressed concrete beams, shear reinforcement, shear strength, cyclic loading, finite element analysis, truss analogy*

1. INTRODUCTION

There have been many studies on shear behavior of concrete beams with shear reinforcement[1]. Based on experimental observation that inclination of diagonal crack at mid height of a beam is around 45°, a truss mechanism with concrete diagonal strut whose angle to member axis is 45° has been used as shear resisting mechanism. Hypothesis that external shear force is balanced by internal shear forces carried by this truss mechanism and carried by other mechanism is widely accepted as in shear strength equations[2),3)]. Experimentally observed relationship between strain of shear reinforcement and external shear force supports the hypothesis[4)].

Several questions concerning the truss mechanism arose after careful experimental observation[5)].

1) Whether it is true that the angle of concrete diagonal strut is 45° since experimentally observed angles of principal compressive strain in concrete are less than 45° and that of diagonal cracks.

2) The shear force carried by the mechanism other than the truss mechanism (or by concrete) is assumed to be shear cracking strength. How can the shear cracking strength which is the shear force carried by concrete before shear cracking be the shear force carried by concrete even after shear cracking? How can the shear force carried by concrete remain constant as external shear force increases?

Besides these questions it is known that the truss mechanism cannot explain relationship between strain of shear reinforcement and external shear force under unloading and reloading.

In this study shear resisting mechanism of concrete linear members with shear reinforcement is thoroughly investigated by a finite element analysis. The finite element analysis program used is an extended version of the nonlinear finite element analysis program for reinforced planar elements, WCOMR[6),7)]. A new truss model is presented to explain shear resisting mechanism under not only loading but also unloading.

2. ANALYZED BEAMS

Three beams BDP10, BMLW and BCW with stirrup were used in this study. Their dimensions and reinforcement arrangements are shown in **Fig.1**.

Table 1 Details of specimens

Specimen	Prestressing force kN	Concrete strength MPa	Effective depth mm	Tension reinforcement ratio %	Shear reinforcement ratio %	Shear span to effective depth tatio	Concrete Cover[2] mm
BDP10	-	39.2	500	3.04	0.50 0.38	1.60	15
BMLW	-	35.3	522	2.57	0.42 0.53	3.16	31.29
BCW	-	47.4	352	2.70	0.19 0.58	3.98 1.99	94
N18	-	29.4	250	1.51	0.10	3.00	42
N24	-	18.4	250	2.27	0.25	3.30	42
T-beam(1st)	-	32.5	660	1.25	0.42 ~ 0.53	10[1]	17
VDS10	-	29.9	440	2.88	0.91 0.33	2.00 4.00	20
BDL6	-	29.4	250	1.51	0.25	3.03	42
TS1	148	40.5	235	0.59	0.87	3.57	17
TS3	46	39.2	235	0.59	0.87	3.57	17

Note : 1) Span to effective depth ratio, l/d 2) Clear cover

Table 2 Material constants of reinforcement

Reinforcement	Specimen	Elastic modulus GPa	Yield strength MPa	Cross-sectional area mm^2
ϕ9	BDP10	173	314	56.7
D10	BDP10	177	343	75.4
D13	BMLW,BCW	184	384	115.0
D16	BMLW	165	333	213.2
D19	BMLW	188	397	285.0
D22	BDP10,BCW	184	345	380.0
D25	BMLW	184	354	488.9
D6	N18,N24	206[1]	380	28.3
D19	N18,N24	206[1]	380	283.5
D13	T-beam	213	348	132.7
D25	T-beam	206[1]	350	490.9
D10	VDS10	167	379	71.3
D13	VDS10	173	376	126.5
D25	VDS10	190	405	506.7
D6	BDL6	200	380	28.3
D19	BDL6	200	380	283.5
ϕ5	TS1,TS3	195	1748	19.6
D10	TS1,TS3	186	454	78.5

Note : 1) The values are not given in the references, so that 206 GPa are assumed.

The stirrups in beams BMLW and BCW were welded to longitudinal reinforcement at both ends to prevent any slip at the ends. Material constants for steel and concrete are given in **Tables 1** and **2**. Three beams were simply supported and loaded statically by a hydraulic jack. Deflections and strains of shear and tension reinforcement were measured.

Six beams with stirrups N18, N24, T-beam (first), VDS10, TS1 and TS3 with stirrups from previous studies[8)-12)] shown in **Fig.2** were analyzed as well. Beams TS1 and TS3 are prestressed concrete beams. Measured stirrup strains and ultimate strengths were compared with the analytical predictions in this study. One sample beam BDL6 shown in **Fig.3** was used solely for the analysis in which strains of stirrup and concrete were carefully examined.

All the specimens were analyzed by a finite element program. Examples of finite element meshes of the beams are shown in **Fig.4**. In this study enforced displacements were given at the loading point and prestressing forces were applied as a load at a node of a steel element attached to the specimens.

3. MODIFIED CONSTITUTIVE MODELS

(1)Need for Expansion of WCOMR

A program, WCOMR, for nonlinear finite element analysis was developed to estimate deformational

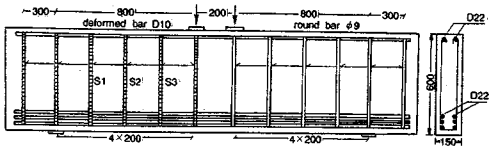

(a) Beam BDP10

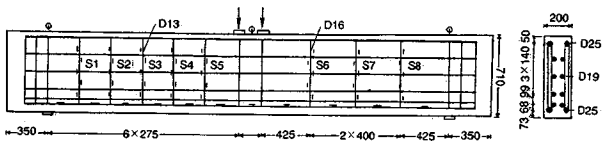

(b) Beam BMLW

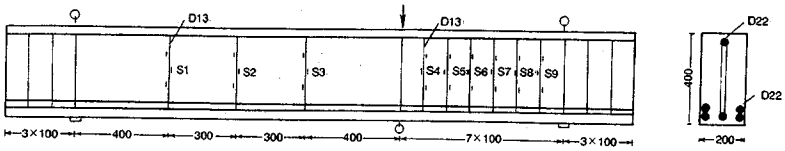

(c) Beam BCW

Fig.1 Analyzed beams

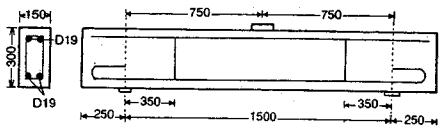

(a) Beam N18[8)]

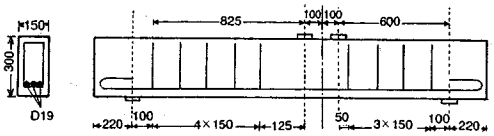

(b) Beam N24[8)]

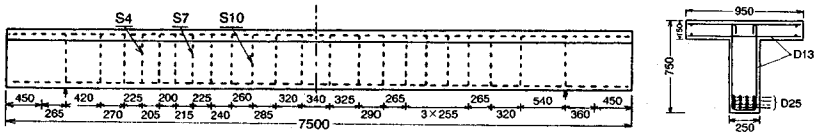

(c) T-beam (first)[9)]

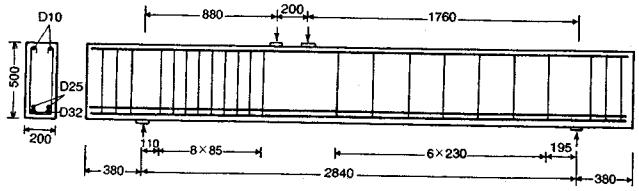

(d) Beam VDS10[10)]

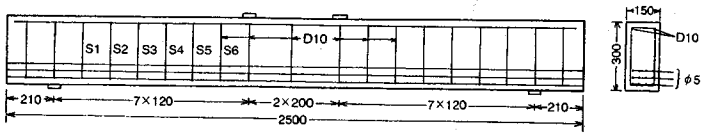

(e) Beams TS1 and TS3[12)]

Fig.2 Analyzed beams taken from previous studies[8)~10),12)]

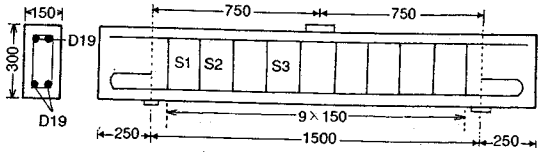

Fig.3 Analyzed beam (beam BDL6)

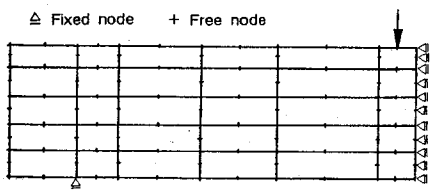

(a) Left shear span of beam BMLW

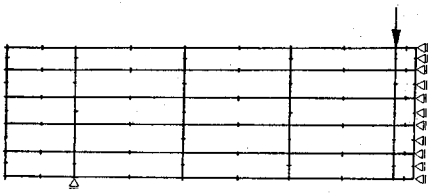

(b) Right shear span of beam BMLW

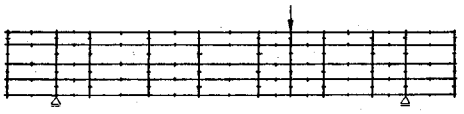

(c) Beam BCW

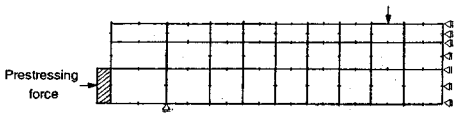

(d) Beams TS1 and TS3

Fig.4 Finite element meshes

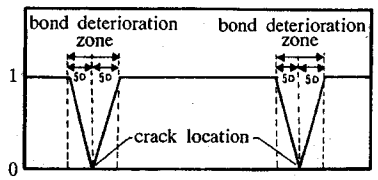

Fig.6 α-diagram

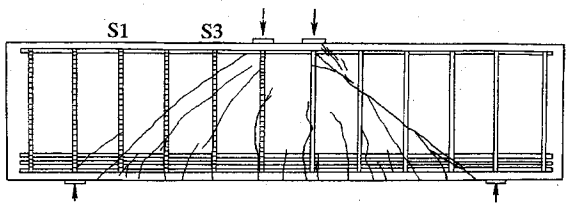

(a) Cracking pattern

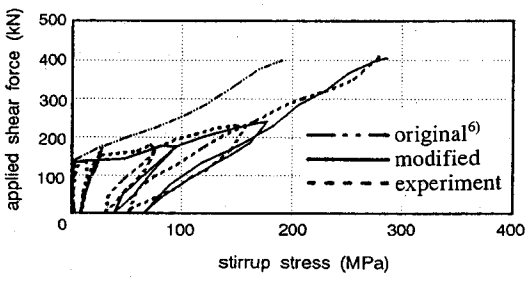

(b) Stirrup S1

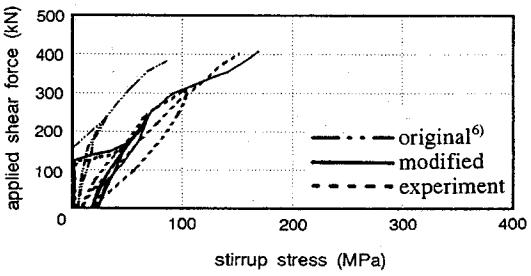

(c) Stirrup S3

Fig.5 Cracking pattern and relationships between shear reinforcement stress and applied shear force in beam BDP10

behavior of reinforced concrete wall under reversed cyclic loading[6),7)]. The program successfully predicts experimentally observed deformations and strengths of walls and has been applied to linear members as well[7),11)]. It is found, however, that WCOMR cannot predict stirrup strains in concrete beams accurately. Discrepancy between the predicted and experimental results is as shown in **Fig.5**.

It is believed that micro-mechanical models (constitutive models) for reinforced concrete walls which are not suitable for beams may have caused the discrepancy. These unsuitable constitutive models are models for tension stiffness of concrete and force transfer at crack.

(2)Modified Model for Tension Stiffness of Concrete

The model for tension stiffness of concrete in WCOMR is provided for cases in which there is no slip at anchorage. In linear members, however, there may be anchorage slips of shear reinforcement.

In a previous study[13)]slips of shear reinforcement at corner bends were found in columns. In another study[10)] it was observed that there were only negligible slips at the hooks of deformed stirrups whereas significant slips were observed at the hooks of plain stirrups in beams. It was also found[10)] that opening of shear crack was caused by not only elongation of the vertical portion of the stirrup but also elongation of its horizontal portion between the lower bends in tension zone. The elongation of the horizontal portion induces slipping upwards at the lower bends. Effect of the slip on the tension stiffness of concrete is investigated below.

Shima et al[14)] show that bond stress-slip relationship between concrete and reinforcement is affected by boundary condition, such as reinforcement stress and slip, and present the bond stress-slip-reinforcement strain relationship, Eq.(1)

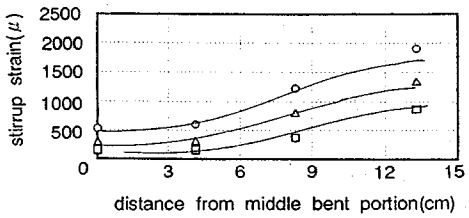

(a) Stirrup S1

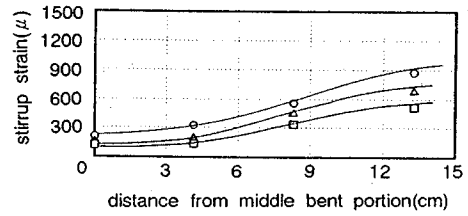

(b) Stirrup S2

Fig.7 Stirrup strain distributions along stirrups in beam BDP10 (β=1.5)

which is a bond stress-slip relationship applicable to any boundary condition.

$$\frac{\tau}{f_c'} = \frac{0.73(\ln(1+5s))^3}{1+\varepsilon_s \times 10^5} \qquad (1)$$

where τ is bond stress, f_c' is concrete compressive strength, $s = 1000(S/D)$ which is slip, S normalized by reinforcement diameter, D, and ε_s is reinforcement strain. Concrete and steel stress distributions along steel reinforcement can be calculated by using Eq.(1) as well as stress-strain relationships of concrete and steel. Eq.(1), however, is only applicable to reinforcement embedded with a large cover and spacing. The cover for the shear reinforcement in beams is usually small. A small cover is expected to reduce the bond stress or the reinforcement strain for the same slip[10]. Another effect to reduce the bond stress is the bond deterioration near the intersection with a crack. A modified relationship, Eq.(2) is obtained to consider the effect of the cover and the crack intersection.

$$\frac{\tau}{f_c'} = \alpha \frac{0.73(\ln(1+5s))^3}{1+\beta\varepsilon_s \times 10^5} \qquad (2)$$

where α and β are coefficients to consider the effects of the crack intersection and the cover respectively. The bond deterioration zone near the crack intersection is assumed to be within distance of $5D$ from the intersection and to be independent of angle between crack and reinforcement[15]. It is assumed that the bond stress is reduced linearly and

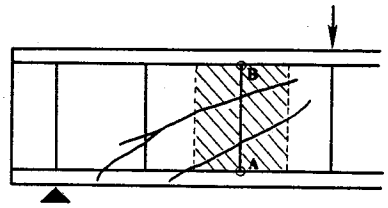

Fig.8 Concrete element around shear reinforcement

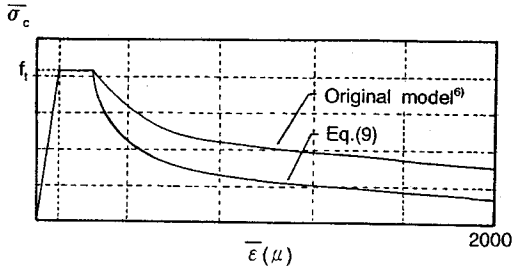

Fig.9 Comparison of modified tension stiffness model with original model[6]

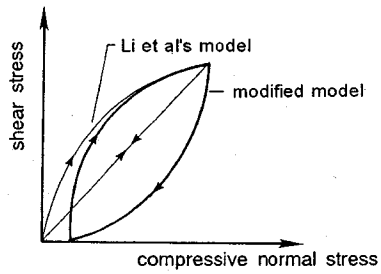

Fig.10 Comparison of modified model for force transfer at crack with original model[17]

is zero at the crack intersection as shown in **Fig.6**. The value of β which is 1.5 is chosen to fit with the measured distributions of stirrup strains as shown in **Fig.7**.

In order to find a tension stiffness model for concrete reinforced with deformed stirrup, relationship between average stress and strain of concrete element indicated by the hatched area in **Fig.8** is calculated as follows. Slip between reinforcement and concrete is defined by Eq.(3).

$$S = \int \varepsilon_s dx + S_0 \qquad (3)$$

where x : distance taken along reinforcement, S_0 : slip at end. Eq.(4) indicating relationship between bond stress and reinforcement strain is derived from an equilibrium between bond force and reinforcement force.

$$\tau = \frac{E_s D}{4} \frac{d\varepsilon_s}{dx} \qquad (4)$$

where E_s : elastic modulus of reinforcement. When

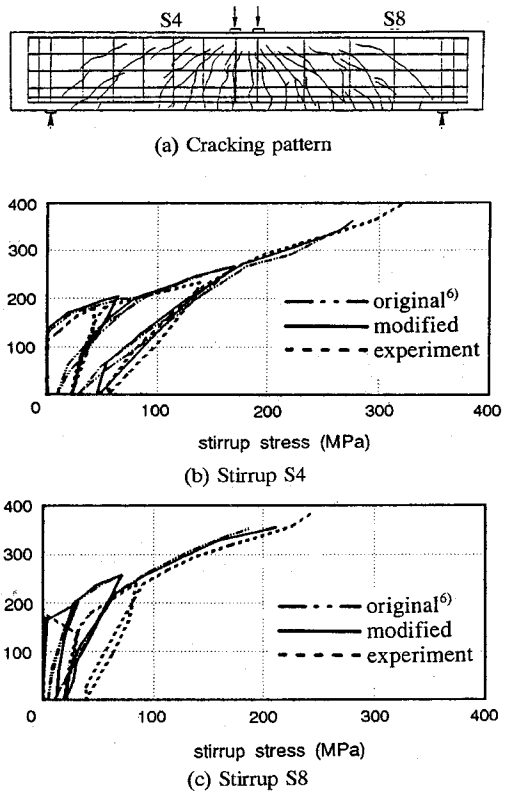

Fig.11 Cracking pattern and relationships between shear reinforcement stress and applied shear force in beam BMLW

a crack opening is small, relationship between concrete tensile stress and crack opening at the crack is expressed by Eq.(5)[16].

$$\frac{\sigma_c}{f_t}=\left[1+\left(c_1\frac{w}{w_0}\right)^3\right]\exp\left(c_2\frac{w}{w_0}\right)-\frac{w}{w_0}(1+c_1^3)\exp(-c_2) \quad (5)$$

where σ_c : concrete stress, f_t : tensile strength of concrete, $w=S_{cr}-\Delta L_c$: crack opening (crack width), $w_0=160\mu m$: crack opening at which concrete tensile stress becomes zero, $c_1=3$ and $c_2=6.93$: material constants, $S_{cr}=\int \varepsilon_s dx+S_0$: slip at crack, $\Delta L_c=\int \varepsilon_c dx$: total concrete deformation, ε_c : strain of the concrete. The slip, S_0 at a lower bent (point A in **Fig.8**) which is obtained by integrating reinforcement strain between the lower bents is given as a function of the reinforcement strain at the lower bent, $f(\varepsilon_s)$ This function is obtained by Eqs.(2) (3) and (4). The slip at a hook (point B in **Fig.8**) is assumed to be zero. Relationships between

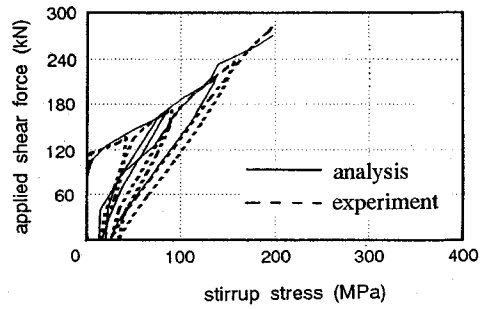

Fig.12 Relationships between shear reinforcement stress and applied shear force in beam BCW (average of stresses in stirrup S4 and S5)

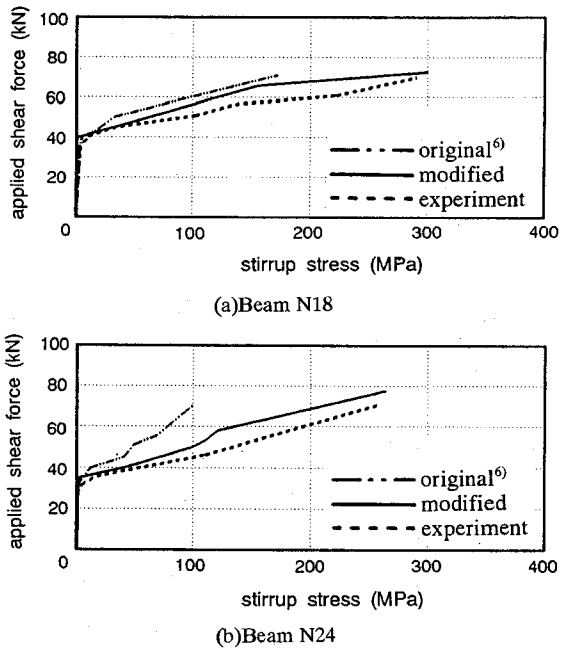

Fig.13 Relationships between shear reinforcement stress and applied shear force in beams N18 and N24[8]

the concrete tensile stress and strain at unloading is assumed to be linear with a stiffness equal to the initial stiffness. Using stress-strain relationship of the reinforcement and the stress-strain relationship of the concrete in tension with Eqs.(2)~(5), strain and stress distributions of the concrete and the reinforcement can be obtained. Average strain and stresses are then calculated as in Eqs.(6)~(8).

$$\bar{\varepsilon}=\bar{\varepsilon}_c=\bar{\varepsilon}_s=\frac{1}{L}\left[\int \varepsilon_s(x)dx+S_0\right] \quad (6)$$

$$\bar{\sigma}_c=\frac{1}{L}\left[\int \sigma_c(x)dx\right] \quad (7)$$

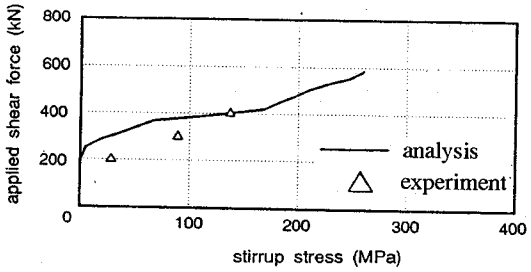

(a) Stirrup S4

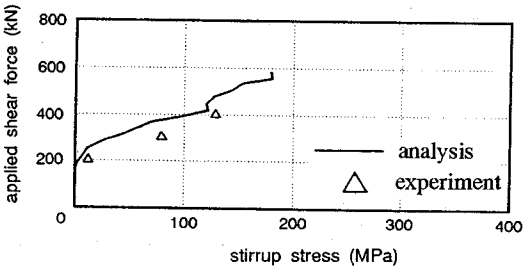

(b) Stirrup S7

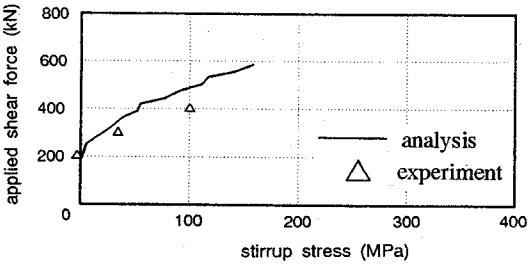

(c) Stirrup S10

Fig.14 Relationships between shear reinforcement stress and applied shear force in T-beam[9]

$$\overline{\sigma_s} = \frac{1}{L}\left[\int \sigma_s(x)\,dx\right] \tag{8}$$

where $\overline{\varepsilon}$, $\overline{\varepsilon_c}$ and $\overline{\varepsilon_s}$: average strains of reinforced concrete, concrete and reinforcement, L : length of a concrete element, $\overline{\sigma_c}$ and $\overline{\sigma_s}$: average stresses of concrete and reinforcement. Relationship between average concrete stress and strain can be expressed approximately by Eq.(9).

$$\overline{\sigma_c} = f_t\left(\frac{\varepsilon_{tu}}{\overline{\varepsilon_c}}\right)^{k_1} \exp\left[-k_2\left(1-\frac{\varepsilon_{tu}}{\overline{\varepsilon_c}}\right)\right] \tag{9}$$

where $\varepsilon_{tu} = 0.02\%$: strain corresponding with concrete tensile strength, $k_1 = 0.3$ and $k_2 = 1$: constants. Eq.(9), which is a modified tension stiffness model, is compared with the original model[6] in **Fig.9**. Effect of the slip at the lower bent

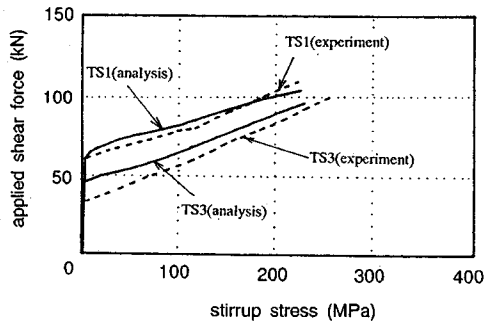

Fig.15 Relationships between shear reinforcement stress and applied shear force in beams TS1 and TS3[12] (average of stresses in stirrup S5 and S6)

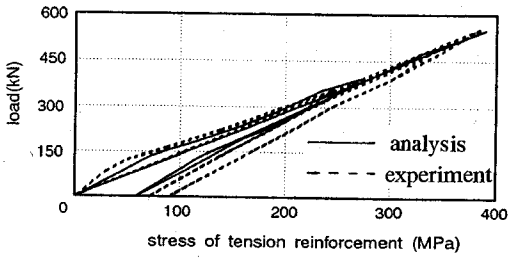

Fig.16 Relationships between tension reinforcement stress and load in beam BMLW

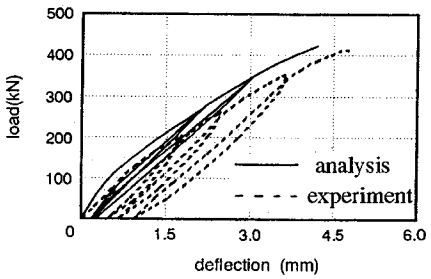

Fig.17 Relationships between deflection and load in beam BCW

is clearly seen in such a way that the modified model gives a stress less than the original model for a given strain.

Effects of number of cracks intersecting the reinforcement and length of concrete element on the average concrete stress-strain relationship were investigated. The stress-strain relationship did not change much between cases of one and two cracks and between cases of the lengths of 300 mm and 600 mm. The effects are considered to be negligible for beams of this size range.

For unloading and reloading, it is assumed that the stress carried by the concrete is a sum of stress transmitted by crack contact, $\overline{\sigma_{cc}}$ and stress by bond, $\overline{\sigma_{cb}}$ as shown in Eq.(10). The same models as in a previous study[14] are applied for $\overline{\sigma_{cc}}$ and $\overline{\sigma_{cb}}$.

Table 3 Ultimate strength of beams

Specimen	Ultimate strength		Failure mode	
	V_{cal}(kN)	V_{exp}(kN)	prediction	experiment
BDP10	392.3	397.5	S-NY-NY[1)2)3)]	S-NY-NY
BMLW	347.2	374.0	F-NY-Y	F-NY-Y
BCW	135.9	138.5	S-NY-NY	S-Y-NY
N24	68.8	75.9	S-NY-NY	F-NY-Y
N18	69.6	81.4	S-NY-NY	S-Y-Y
T-beam	589.6	519.8	S-NY-NY	S-Y-NY
TS1	103.8	107.9	F-NY-NY	F-NY-NY
TS3	95.0	100.5	F-NY-NY	F-NY-NY

Note : 1) S=shear failure F=flexure failure
2) Y and NY = yielding and no yielding of shear reinforcement
3) Y and NY = yielding and no yielding of tension reinforcement

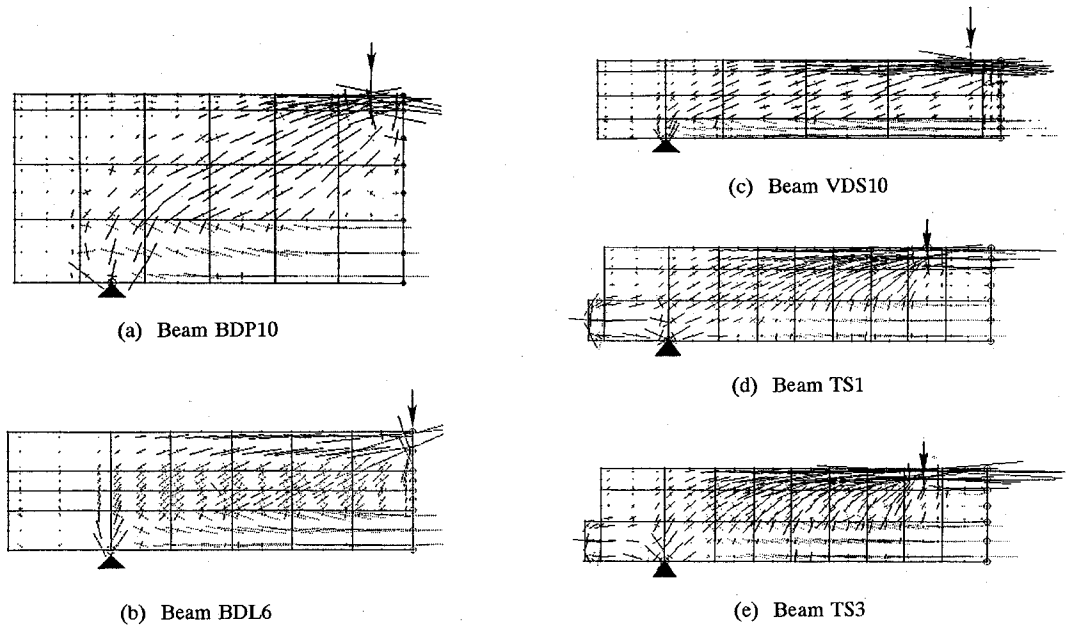

(a) Beam BDP10

(b) Beam BDL6

(c) Beam VDS10

(d) Beam TS1

(e) Beam TS3

Fig.18 Concrete stress flow in a shear span

$$\overline{\sigma_c} = \overline{\sigma_{cc}} + \overline{\sigma_{cb}} \qquad \textbf{(10)}$$

It was found that relationship between the average reinforcement stress and strain was not influenced much by the slip at the lower bent, the number of the cracks nor the length of the concrete element. Therefore, the original model for the average reinforcement stress and strain curve is applied.

(3)Modified Model for Force Transfer at Crack

A model for force transfer at crack in WCOMR[6),7)] is based on Li et al's model[17)] which was obtained using mostly data of experiment in which crack openings were kept constant as shear slips changed. The Li et al's model is expressed by Eqs.(11) and (12).

$$\tau_c = 3.83 f_c'^{1/3} \frac{\lambda^2}{1+\lambda^2} \qquad \textbf{(11)}$$

$$\sigma_c' = 3.83 f_c'^{1/3} \left[\frac{\pi}{2} - \cot^{-1}\lambda - \frac{\lambda}{1+\lambda^2} \right] \qquad \textbf{(12)}$$

where τ_c : shear stress along a crack, σ_c' : compressive stress normal to a crack, f_c' in MPa, $\lambda = \frac{\delta}{w} = \frac{\gamma_{xy}}{\varepsilon_x}$, δ : shear slip along a crack.

In beams, however, crack openings change as shear slips change[18)]. In order to investigate

applicability of the Li et al's model to beams, shear and normal stresses transferred at shear cracks were calculated from the measured crack openings and shear slips using Bujadham et al's model[15], a modified Li et al's model applicable to any loading path. At loading (envelope curve) the shear stresses calculated by the Li et al's model are slightly greater than those by the Bujadham et al's model. Shear stress-normal compressive stress relationships at unloading and reloading (inner curve) are quite different between cases of the Li et al's model and the Bujadham et al's model. Considering dowel action which is not considered in the Li et al's model, the Li et al's model is used at loading while the shear stress-normal compressive stress relationships at unloading and reloading are modified as follows (see **Fig.10**).

$$\frac{\tau_c}{\tau_{max}} = \left(\frac{\sigma_c'}{\sigma_{max}'} \right)^k \qquad (13)$$

$$\frac{\sigma_c' - \sigma_{min}'}{\sigma_{max}' - \sigma_{min}'} = \left(\frac{\tau_c - \tau_{min}}{\tau_{max} - \tau_{min}} \right)^k \qquad (14)$$

where τ_{max}, σ_{max}', τ_{min} and σ_{min}' : maximum and minimum shear and normal compressive stresses at last loading, $k = 5$: a constant.

4.VERIFICATION FOR MODIFIED MODELS

Cracking pattern and relationships between shear reinforcement stress and applied shear force in beam BDP10 are shown in **Fig.5**. The relationships calculated by the original models fail to predict the observed relationships at both envelope and inner curves. At the envelope the predicted shear reinforcement stresses are clearly less than the observed ones for the same applied shear forces. The remaining stresses of the shear reinforcement are also less than the observed ones. On the other hand the relationships calculated by the finite element analysis with the modified models agree well with the observed ones at their envelopes as well as the inner curves.

Figs.11 and **12** indicate relationships between shear reinforcement stress and applied shear force in beams BMLW and BCW. Cracking pattern in beam BMLW is given also in **Fig.11**. It can be seen in **Fig.11** that the relationships calculated by the original models predict well at the envelope part but underestimate significantly the remaining shear reinforcement stresses. In beams BMLW and BCW there should be no slip at the ends of shear reinforcement because all the shear reinforcement was welded to the longitudinal reinforcement. The

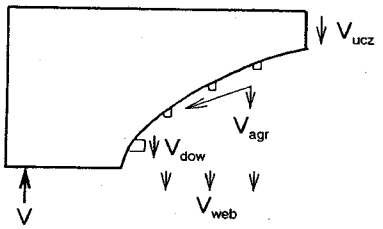

Fig.19 Internal shear forces

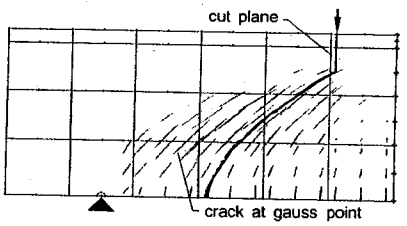

(a) Beam BDP10

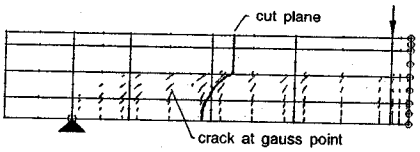

(b) Beam VDS10

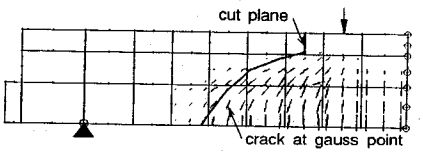

(c) Beam TS1

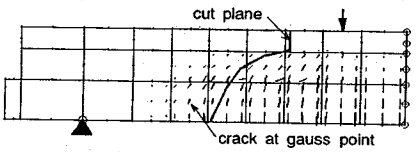

(d) Beam TS3

Fig.20 Cracking patterns and cut planes

effect of the end slip on tension stiffness of concrete does not exist. From the finite element analysis it was found that the model for the tension stiffness of concrete affects the relationship between the shear reinforcement stress and the applied shear force at the envelope part only. It can be said, therefore, that the original models predict well at the envelope part.

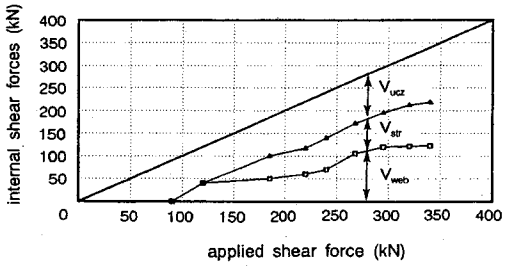

(a) Beam BDP10

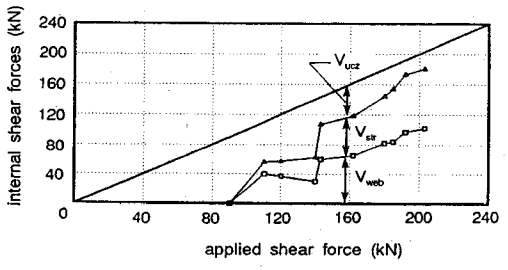

(b) Beam VDS10

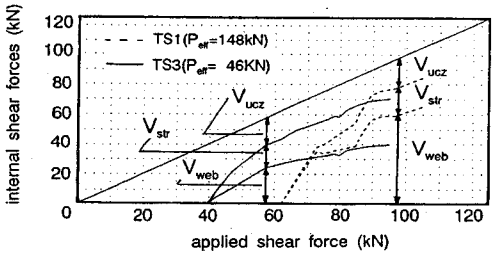

(c) BeamTS1 and TS3

Fig.21 Variation of internal shear forces at loading

The finite element analysis indicates that the inner curves are influenced by the model for the force transfer at crack. The finite element analysis with only the modified model for the force transfer predict well the observed results at both the envelope and the inner curves in **Figs.11** and **12**.

The concrete cover in beam BMLW was much smaller than that in beam BCW. The experimental results in **Figs.11** and **12** do not indicate the effect of the concrete cover, which agrees with the fact that the tension stiffness (Eq.(9)) is hardly affected by concrete cover although the bond-slip-strain (Eq.(2)) is affected.

The finite element analysis with the modified models was also applied to beams in previous studies. Shear reinforcement stress-applied shear force relationships for rectangle beams in Yoshida's study[8] and a T-beam in Farghaly and Okamura's study[9] can be predicted well by the modified models as shown in **Figs.13** and **14**. The finite element program with the modified models can also predict

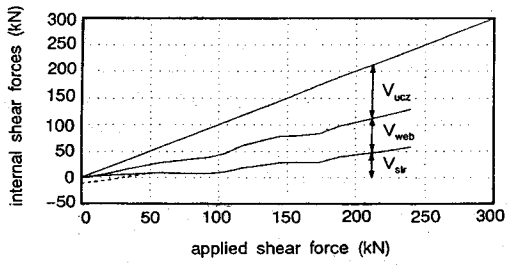

Fig.22 Variation of internal shear forces at unloading

the stirrup stresses in prestressed concrete rectangle beams[12] as shown in **Fig.15**.

It is found that the finite element program with the modified models can predict strains of longitudinal reinforcement and deflection as seen in **Figs.16** and **17**. Predicted and experimentally observed ultimate strengths and failure modes are compared in **Table 3**. The predicted ones agree well with the observed ones in most of the cases.

5. SHEAR RESISTING MECHANISM

Principal stresses of concrete calculated by the finite element program are as shown in **Fig.18**. In a shear span angles of the compressive stresses to the member axis are approximately the same at mid height region (above tension reinforcement level and below compression zone). In slender beams BDL6 and VDS10 (their shear span to effective depth ratios, a/d are 3.0 and 4.0) the angles of the compressive stresses are around 30°. In a deep beam BDP10 (a/d is 1.6) the angles of the compressive stresses are slightly greater than those in the slender beams. In prestressed concrete beams TS1 and TS3 (a/d is 3.57) the greater prestress (beam TS1) gives slightly smaller angles than those with the less prestress (beam TS3).

Shear resisting forces are a shear force carried by uncracked zone, V_{ucz}, a shear force carried by shear reinforcement and concrete surrounding the shear reinforcement (concrete tension stiffness), V_{web} and a shear force carried by other than V_{web} along a shear crack, V_{str} (shear force carried by aggregate interlocking, V_{agr} plus shear force carried by dowel action, V_{dow}) as shown in **Fig.19**. In the finite element analysis, those internal forces were calculated using stresses at the gauss points along a cut plane as shown in **Fig.20**. The internal force, V_{ucz} was obtained at the gauss points above cracking zone (vertical part of the cut plane) and the internal

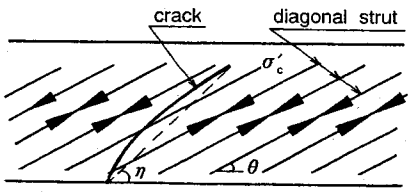

Fig.23 Concrete diagonal strut

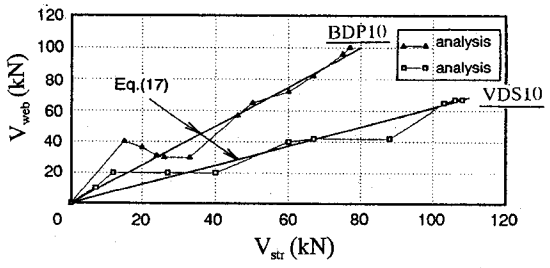

(a) Beams BDP10 and VDS10

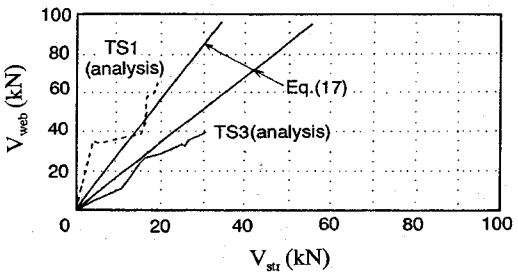

(b) Beams TS1 and TS3

Fig.24 Relationships between shear forces carried by shear reinforcement and aggregate interlocking

forces, V_{web} and V_{str} were obtained at the gauss points within the cracking zone. The internal forces were calculated by multiplying the stresses at each gauss point by area covered by the gauss point. **Fig. 21** shows how the calculated internal forces vary as applied shear force increases. The internal forces, V_{web} and V_{str} increase. The internal force, V_{ucz} carried by the uncracked zone decreases in beam VDS10 and increases slightly in beam BDP10. From **Fig.21 (c)** it is clearly seen that the shear cracking load at which the internal forces, V_{web} and V_{str} start to increase is larger for the greater prestressing force. The internal shear force, V_{web} in beam TS1 is larger than that in beam TS3 and the internal force, V_{str} in beam TS1 is smaller than in beam TS3 at ultimate stage since the shear crack angles are smaller for the greater prestressing force as shown in **Fig.20**.

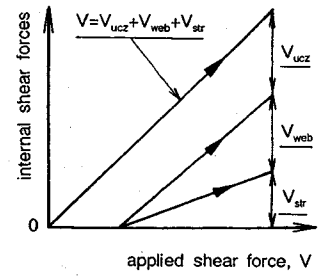

(a) At loading

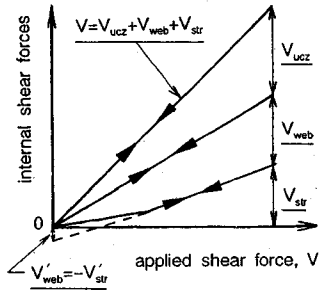

(b) At unloading and reloading

Fig.25 Variation of internal shear forces

Fig.22 shows the variation of the calculated internal forces at unloading in beam BDP10. In this study the internal force, V_{web} is defined as a summation of the shear forces carried by shear reinforcement and by concrete. The shear force carried by the concrete becomes negative for small applied shear forces because concrete compressive stresses are transferred by contacting shear crack surfaces (see Eq.(10)). If the internal shear force, V_{web} is recalculated by subtracting the compressive force due to the crack contact from the original V_{web} and the internal shear force, V_{str} by adding the compressive force due to the crack contact, the relationships between the applied shear force and V_{web} and V_{str} are expressed by dotted line in **Fig.22**.

The observed concrete compressive stress flow can be modeled as diagonal struts with a constant angle, θ which is seen in a conventional truss model (see **Fig.23**). From the truss model the following expressions for the internal forces are derived.

$$V_{dcz} = V_{web} + V_{str} = \sigma_c' b z \cos\theta \sin\theta \qquad (15)$$

$$V_{str} = \sigma_c' b \frac{z}{\sin\eta} \sin(\eta - \theta) \sin\theta \qquad (16)$$

where V_{dcz} : shear force transferred along a shear crack, σ_c' : concrete diagonal compressive stress, b

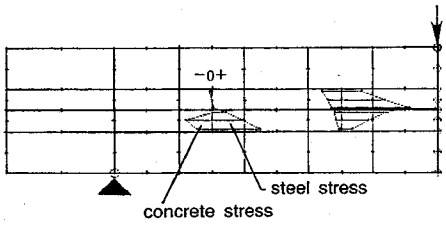

Fig.26 Remaining stresses in a shear span at complete unloading in beam BDL6

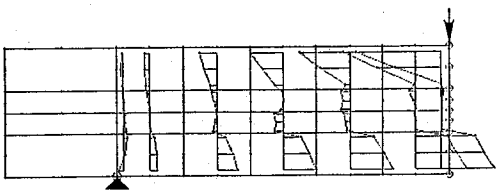

(a) Case with shear cracks

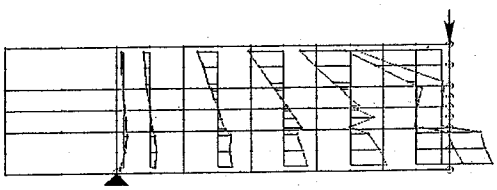

(b) Case without shear cracks

Fig.27 Distributions of normal stress in planes normal to member axis in beam BDL6 (normal stress = concrete stress + reinforcement stress)

: beam web width, z : arm length of truss (distance between compressive force in compression zone and tensile force in tension zone), η : angle of a shear crack. From Eqs.(15) and (16) the following equation is derived.

$$\frac{V_{web}}{V_{str}} = \frac{\cos\eta \sin\theta}{\sin(\eta-\theta)} = \frac{\cot\eta}{\cot\theta-\cot\eta} \qquad (17)$$

Eq.(17) indicates that the ratio of the shear force carried by shear reinforcement and surrounding concrete to the shear force carried by other than those is constant. The ratios of V_{str} to V_{web} calculated by the finite element analysis are more or less constant as predicted by Eq.(17) (see **Fig.24**).

In the finite element analysis the internal shear forces change at unloading and reloading as shown in **Fig.25**. **Fig.25(a)** indicates a situation immediately before the unloading starts. The internal shear force carried by uncracked zone, V_{ucz} as well as the shear force carried by shear

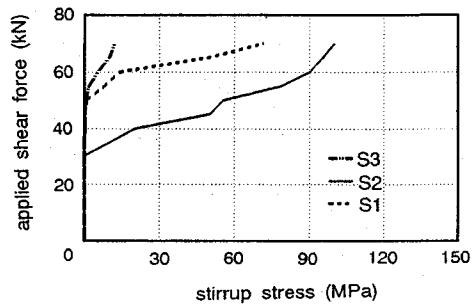

Fig.28 Stresses of shear reinforcement at different locations in beam BDL6

reinforcement and surrounding concrete, V_{web} and the shear force carried by the other, V_{str} decrease nearly proportionally to applied shear force and is close to zero at complete unloading (solid lines in **Fig.25(b)**). The shear reinforcement has remaining stresses. However, the concrete stresses predicted by the tension stiffness model given by Eq.(10) are negative because of crack contact. Therefore the internal force, V_{web} becomes zero at the complete unloading.

A dotted line in **Fig.25(b)** shows variation of the internal shear forces in case where the internal force, V_{web} is recalculated by subtracting the compressive force transferred by the crack contact from the original V_{web} and the internal force, V_{str} by adding the compressive force due to the crack contact. In this case the internal force, V_{web} decreases also linearly but remains at a certain value at the complete unloading. The internal force, V_{str} becomes negative and balances with the remaining V_{web} (see **Fig.25(b)**). **Fig.26** shows the remaining concrete compressive stresses and reinforcement tensile stresses in vertical direction at two gauss points.

Calculated normal stress distributions along planes normal to member axis in a model beam BDL6 are as shown in **Fig.27(a)**. The calculated normal stress distributions in the same beam, in which shear cracking is not made to occur but flexure cracking is, are given in **Fig.27(b)**. The normal stress distributions in **Fig.27(b)** are close to those predicted by a conventional bending theory. Neutral axis depth in **Fig.27(a)** is shallower than that in **Fig.27(b)**. The following facts in **Fig.27(a)** agree with what the truss model predicts : (a) some compressive stresses are seen at mid height, (b) compressive stresses in compression zone are less than those predicted by the bending theory, and (c) tensile stresses in tension zone are greater than those predicted by the bending

theory. **Fig.27** clearly indicates that shear cracking makes the bending theory no longer applicable and introduces a truss-like mechanism in a shear span.

Stresses of shear reinforcement are caused by the truss mechanism. However, it is known that shear reinforcement stresses in the vicinity of loading point and support are less than those in the other region. The finite element analysis predicts this fact in beam BDL6 as shown in **Fig.28**. Greater contribution of concrete tension stiffness due to a delay in shear crack propagation near the loading point and support lessens the shear reinforcement stresses.

6. CONCLUSIONS

Based on analyses with a nonlinear finite element program, WCOMR for reinforced concrete planner members and experiment of beams with shear reinforcement, the followings are concluded on shear resisting mechanism of reinforced and prestressed concrete beams with shear reinforcement under one-sided cyclic loading:

(1)Concrete tension stiffness around shear reinforcement is reduced significantly because of slip at the lower bent of the shear reinforcement. Therefore, the model for the concrete tension stiffness in WCOMR may not be applied to beams with shear reinforcement.

(2)Stresses transferred along shear cracks at unloading and reloading in beams are different from what the model for force transfer at crack in WCOMR.

(3)Modified models for the concrete tension stiffness and the force transfer at crack are presented for analysis of beams with shear reinforcement.

(4)The finite element program with the modified constitutive models can predict well relationship between shear reinforcement stress and applied shear force which cannot be predicted by the program without the modification.

(5)The concrete tension stiffness influences the relationship between shear reinforcement stress and applied shear force at its envelope part. A less concrete tension stiffness causes greater shear reinforcement stresses.

(6)As shear resisting mechanism, a truss-like mechanism is formed in a shear span. The truss mechanism is characterized by uniform diagonal concrete compressive stress flow (diagonal compression strut) with an angle less than 45°.

(7)A shear force carried by the truss mechanism can be divided into two shear force components carried by shear reinforcement and its surrounding concrete, V_{web} and by other, V_{str} which is mainly aggregate interlocking. Those two shear force components increase rather linearly as applied shear force increases. A shear force carried by other than the truss mechanism, V_{ucz} is a shear force carried by uncracked concrete above shear cracking zone.

(8)The internal shear forces, V_{ucz}, V_{web} and V_{str} decrease rather linearly during unloading and become negligibly small at complete unloading. Shear force carried by the shear reinforcement alone remains at the complete unloading. Shear force carried by compressive force due to crack contact exists at the complete unloading to balance with the remaining shear force by the shear reinforcement.

(9)Under effect of prestressing force, angle θ of the uniform diagonal compression stress flow and angle η of shear crack become small. Because of the small η, a ratio of the internal shear force, V_{web} to V_{str} becomes large.

(10)Shear cracking introduces the truss mechanism and reduces depth of flexural compression zone. Because of the truss mechanism compressive stresses in the compression zone decrease and tensile stresses in tension zone increase.

(11)Less stresses of the shear reinforcement near a loading point and a support than in other region are due to greater contribution of the concrete tension stiffness around the shear reinforcement.

ACKNOWLEDGEMENTS: The authors would like to express their gratitude to Prof Hajime Okamura of University of Tokyo and Prof Yoshio Kakuta of Hokkaido University for their valuable comments to this study.

REFERENCES

1) For example,
Okamura, H., Farghaly, S. and Ueda, T. : Behaviors of Reinforced Concrete Beams with Stirrups Failing in Shear under Fatigue Loading, *Proc. of JSCE*, No.308, pp.102~122, April 1981.

2) JSCE Concrete Committee : Standard Specification for Design and Construction of Concrete Structures -1986, Part 1 (Design), JSCE, 1986.

3) ACI Committee 318 : Building Code Requirements for Reinforced Concrete and Commentary - ACI318-89, ACI, 1989.

4) Ueda, T. and Okamura, H. : Behavior in Shear of Reinforced Concrete Beams under Fatigue Loading, *Concrete Library International*, JSCE, Vol.2, pp.37~69, December 1983.

5) Ueda, T., Hassan, H. M. and Koshiji, T. : Shear Resistant Mechanism of Beam with Shear Reinforcement, *Proc. of 12th Conference on Our World of Concrete and Structures*, pp.143~155, August 1987.

6) Okamura, H. and Maekawa, K. : Nonlinear Analysis and Constitutive Models of Reinforced Concrete, *Gihodo Shuppan*, May 1991.

7) Shin, H.M. : Finite Element Analysis of Reinforced Concrete Members Subjected to Reversed Cyclic In-Plane Loadings, Doctoral Dissertation, The University of Tokyo, June 1988 (in Japanese).

8) Yoshida, T. : A Study on Shear Behavior of Reinforced Concrete Beams, Master Thesis, Nagaoka University of Technology, March 1986 (in Japanese).

9) Okamura, H. and Farghaly, S. : Shear Design of Reinforced Concrete Beams for Static and Moving Loads, *Proc. of JSCE*, No.287, pp.127~136, July 1979.
10) Hassan, H. M., Farghaly, S. and Ueda, T. : Displacements at Shear Crack in Beams with Shear Reinforcement under Static and Fatigue Loadings, *Proc. of JSCE*, No.433/V-15, pp.215~222, August 1991.
11) Koshiji, T. and Okamura, H. : The Effect of Cyclic Loading on Shear Resisting Mechanism in RC Beams, *Proc. of JCI*, Vol.11, No.2, pp.339~344, June 1989 (in Japanese).
12) Ueda, T., Lorenzo, J. N. and Hassan, H. : Effects of Prestressing Force on Mechanical Behavior in Shear of Prestressed Concrete Beams, *Proc. of EASEC-2*, Vol.3, pp.161~166, January 1989.
13) Kameda, T. and Ogura, K. : Experimental Study on Anchorage Capacity of Various Hook Shapes for Shear Reinforcement Bars of R.C. Members, *Proc. of JCI*, Vol.8, pp.601~604, June 1986 (in Japanese).
14) Shima, H. and Okamura, H. : Micro and Macro Models for Bond Behavior in Reinforced Concrete, *Journal of the Faculty of Engineering*, The University of Tokyo(B), Vol.39, No.2, pp.133~194, September 1987.
15) Bujadham, B. and Mishima, T. : Cyclic Discrete Modeling for Reinforced Concrete, *Proc. of SCI-C* 1990, Second International Conference, pp.1225~1236, April 1990.
16) Reinhardt, H.W., Cornelissen, H.A.W. and Hordijk, D.A. : Tensile Tests and Failure Analysis of Concrete, *Journal of Structural Engineering*, ASCE, pp.2462~2477, November 1986.
17) Li, B., Maekawa, K. and Okamura, H. : Contact Density Model for Stress Transfer across Crack in Concrete, *Journal of the Faculty of Engineering*, The University of Tokyo (B), Vol.40, No.1, pp.9~52, March 1989.
18) Hassan, H.M. : Shear Cracking Behavior and Shear Resisting Mechanism of Reinforced Concrete Beams with Web Reinforcement, Doctoral Dissertation, The University of Tokyo, March 1988.

(Received August 1, 1994)

せん断補強されたはりのせん断抵抗機構の有限要素解析

上田多門・Nares　Pantaratorn・佐藤靖彦

正負交番荷重を受ける鉄筋コンクリート面部材用の非線形有限要素解析プログラムを，一方向に繰り返し荷重を受ける鉄筋コンクリート及びプレストレストコンクリート棒部材の解析用に拡張している．元々のプログラムでは精度良く推定できなかったせん断補強筋の歪み挙動を，せん断補強筋の曲げ成形部での滑りによる周囲コンクリートの引張剛性の低下等を考慮することにより，精度良く推定できることを示している．終局耐力も有限要素解析によって妥当に推定できる．以上の解析結果に基づき，せん断補強されたはりのせん断抵抗機構を説明できる新しいトラスモデルを提示している．